UC Santa Cruz

Title
Systematic Design of Space-Time Convolutional Codes

Permalink
https://escholarship.org/uc/item/4vb8k3xr

Author
Rouchy, Christophe L.

Publication Date
2014

Peer reviewed|Thesis/dissertation

UNIVERSITY OF CALIFORNIA

SANTA CRUZ

Systematic Design of Space-Time Convolutional Codes

A thesis submitted in partial satisfaction

of the requirements for the degree of

MASTER OF SCIENCE

in

ELECTRICAL ENGINEERING

by

Christophe Rouchy

March 2014

The Thesis of Christophe Rouchy

is approved:

_____
Professor Hamid Sadjadpour, Chair

_____
Professor J. J. Garcia-Luna-Aceves

_____
Professor Dowla Farid U.

_____

Tyrus Miller

Vice Provost and Dean of Graduate Studies

Contents

List of Figures

List of Tables

Standard Notation

$\lVert \cdot \rVert$	Euclidean norm
$\lVert \cdot \rVert_F$	Frobenius norm
$*$	Conjugate
det	Determinant of a matrix
H	Hermetian
I_N	$N \times N$ Identity matrix
Tr	Trace of a matrix

Space-Time Coding Notation

h_{n_T,n_R}	Path gain from transmit antenna n_T to receive antenna n_R
b	Number of transmit bits per channel use
d_{min}	Minimum distance
E_s	Average power of transmitted symbols
f_d	Doppler shift
G_c	Coding gain
G_d	Diversity gain
H	$n_R \times n_T$ channel matrix
n_R	Number of receive antennas
n_T	Number of transmit antennas

Abbreviations

AWGN	Additive White Gaussian Noise
BER	Bit Error Rate
BW	Band Width
BLAST	Bell Labs Layered Space-Time
BPSK	Binary Phase Shift Keying
CAP	Combined Array Processing
D-BLAST	Diagonal Blast
FER	Frame Error Rate
H-BLAST	Horizontal BLAST
LOS	Line Of Sight
MIMO	Multiple-Input Multiple-Output
MISO	Multiple-Input Single-Output
M-QAM	Multi-Level Quadrature Amplitude Modulation
MRC	Maximal Ratio Combining
MTCM	Multiple Trellis Coded Modulation
OFDM	Orthogonal Frequency Division Multiplexing
PEP	Pairwise Error Probability
PSK	Phase Shift Keying
QAM	Quadrature Amplitude Modulation

QPSK	Quadrature Phase Shift Keying
RF	Radio Frequency
Rx	Receiver
SISO	Single-Input Single-Output
SIMO	Single-Input Multiple-Output
SM	Spatial Multiplexing
SNR	Signal to Noise Ratio
SOSTTC	Super-Orthogonal Space-Time Trellis Code
ST	Space-Time
STBC	Space-Time Block Code
STBC-MTCM	Space-Time Block Code Multiple Trellis Coded Modulation
STCC	Space-Time Convolutional Code
STTC	Space-Time Trellis Code
TCM	Trellis Coded Modulation
Tx	Transmitter
V-BLAST	Vertical BLAST

Abstract

Christophe Rouchy

Systematic Design of Space-Time Convolutional Codes

Space-time convolutional code (STCC) is a technique that combines transmit diversity and coding to improve reliability in wireless fading channels. In this proposal, we demonstrate a systematic design of multi-level quadrature amplitude modulation (M-QAM) STCCs utilizing quadrature phase shift keying (QPSK) STCC as component codes for any number of transmit antennas. Moreover, a low complexity decoding algorithm is introduced, where the decoding complexity increases linearly by the number of transmit antennas. The approach is based on utilizing a group interference cancellation technique also known as combined array processing (CAP) technique.

Finally, our research topic will explore:

- with the current approach, a scalable STTC with better performance as compared to space-time block code (STBC) combined with multiple trellis coded modulation (MTCM) also known as STBC-MTCM;

- the design of low complexity decoder for STTC;

- the combination of our approach with multiple-input multiple-output orthogonal frequency division multiplexing (MIMO-OFDM).

Chapter 1

Introduction

Space-time code [1] has demonstrated remarkable performance by combining the capabilities of transmit spatial diversity with coding. In its original design, the space-time code required multiple transmit antennas in order to transmit encoded symbols simultaneously from different transmit antennas. In this paper, we present a technique that allows us to employ STCC to systems with only a single transmit antenna and multiple receiver antennas. The idea is to transmit more than one symbol from a single transmit antenna. We first present a technique that combines multiple symbols required to transmit in space-time code by superimposing them on each other. In order to combine these symbols at the transmitter and be able to separate them at the receiver, we multiply each symbol by different values that is known at the receiver, and then combine them. Therefore, many symbols can be sent out from a single transmit antenna in one symbol time period. This approach can be interpreted as creating additional transmit antennas, called virtual antennas. These virtual antennas create statistically dependent channels between virtual transmit antennas and each receive antenna that we call virtual

1

paths. Once we show that one can transmit multiple symbols generated from the output of the STCC encoder using a single transmit antenna, we then demonstrate that a multiple-input multiple-output (MIMO) $n_T \times n_R$ system can be modeled equivalently with n_T distinct $1 \times n_R$ single-input multiple-output (SIMO) systems and apply STCC for each of $1 \times n_R$ SIMO systems. This approach allows us to use QPSK STCCs as component codes and create STCCs with arbitrary high spectral efficiencies.

It has been shown in [2, 3, 4] that any M-QAM symbols with square constellation can be constructed with $\frac{\log_2 M}{2}$ QPSK symbols. This unique construction of M-QAM symbols is obtained by rotation and scaling of QPSK symbols using different scaling factors. In this thesis, we construct M-QAM STCC utilizing QPSK STCC as component codes. This construction will allow us to have any M-QAM STCC constellation with a single QPSK STCC encoder.

1.1   Outline

This thesis is organized as follows. Chapter 2 summarizes the works that are directly related to our research and introduce the models used throughout the text. Chapter 3 presents the preliminary work done on Space-Time Convolutional Code. Specifically, the preliminary works can be divided into three parts:

- First, we derive the upper bound pairwise block error probability (PEP) of the M-QAM system (built from QPSK signal) to evaluate the performance and compare with the original STCC design.

- Second, we demonstrate, through simulation results, that the new scheme,

combining 2 QPSK STCCs, outperforms the existing 16-QAM STCC of [1].

- Finally, we present a comprehensive analysis of soft decoding combined array processing (CAP) for STCC and show that we are only 0.5 dB away from the 16-QAM reference but with a lower decoder complexity.

In Chapter 4, we propose a future research topic along the line of designing a scalable STCC, low complexity decoder, with better performance as compared to space-time block code (STBC) combined with multiple trellis coded modulation (MTCM) also known as STBC-MTCM. Finally, we conclude this thesis in Chapter 5.

Chapter 2

Related Work and System Models

This chapter summarizes the main results reported in the literature on the field of Space-Time Convolutional Code that are related to our studies. The models and fundamental assumptions employed throughout the thesis are also described here.

2.1 Wireless Channels

Wireless channels have different paths between the transmitter and receiver. The receiver will be receiving different version of the transmitted signal with multiple phases and amplitudes (see figure 2.1 from [13]).

MIMO systems exploit the spatial dimension (multiple antennas) to improve:

- spectral efficiency in bps/Hz;

- quality (bit error rate (BER)/frame error rate (FER)/outage).
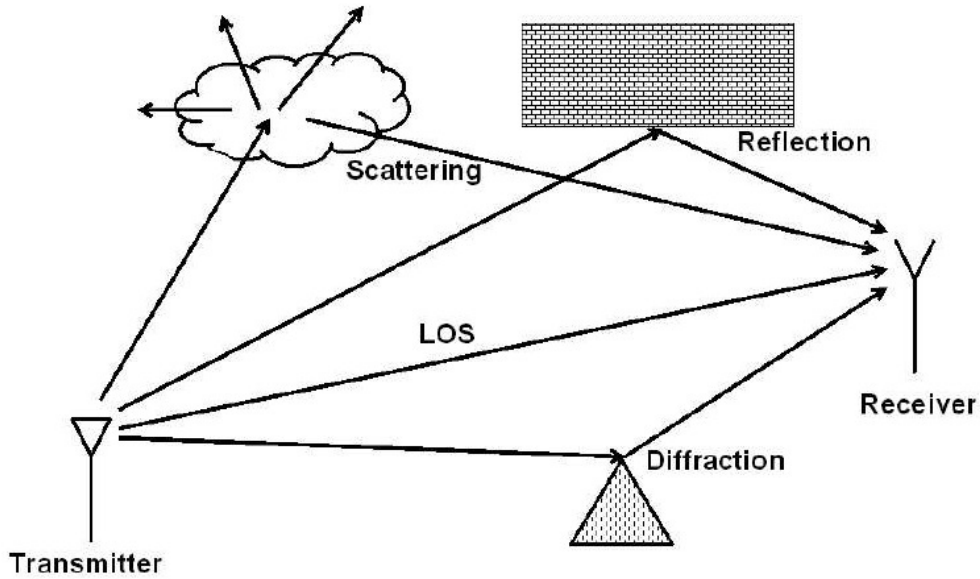
Figure 2.1: An example of different paths in a wireless channel

The following figure from [15] describes different antenna configurations for a wireless system.

If we assume for a SISO system that there is no line of sight (LOS) path between the transmit and receive antenna, flat fading and the impulse responses of multi path channel are random, the receive signal is given by

$$r_t = h_{11}c_t + n_t, \qquad (2.1)$$

where h_{11} (the path gain between transmit antenna 1 and receive antenna 1) is a complex Gaussian random variable, c_t is the transmitted signal and n_t is a Gaussian noise.
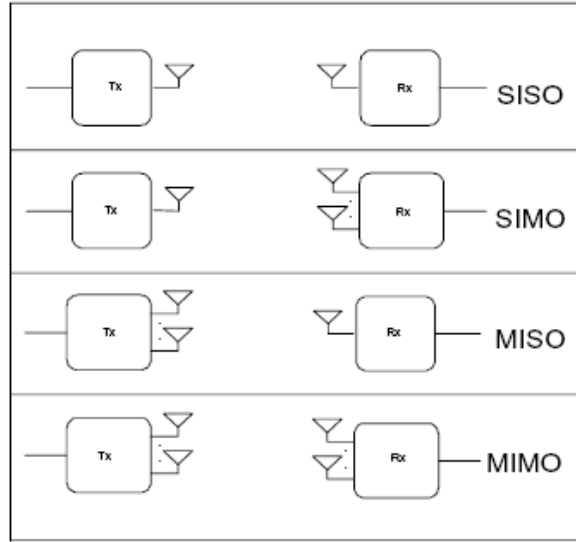
Figure 2.2: An example of different antenna configurations for a wireless channel

2.2 Diversity

In case of fading channel, the receiver can see deep fade which can cause outage. Spatial diversity can be seen as having different copy of the transmit signal to the receiver. Diversity reduces the probability of having all the copies in deep fade.

The diversity definition is given by the following formula

$$G_d = - \lim_{\gamma \to \infty} \frac{\log(P_e)}{\log(\gamma)}, \tag{2.2}$$

where P_e is the error probability at SNR of γ. The diversity can be seen as the slope of the curve FER versus SNR when plotted in a log-log scale.

2.3 Capacity of MIMO channels

The capacity of MIMO channels has been investigated in [16] and [17]. The capacity gives the maximum error free data rate. We assume that the receiver knows the realization of the channel H but not the transmitter (open loop system). For a MIMO system with n_T transmit antennas and n_R receive antennas, the input-output relation is defined as

$$\mathbf{r} = \mathbf{Hc} + \mathbf{n} \tag{2.3}$$

where $\mathbf{r}$ is the $n_R \times 1$ received signal vector, $\mathbf{c}$ is the $n_T \times 1$ transmitted signal vector and $\mathbf{n}$ is the Gaussian noise.

For a deterministic MIMO channel, the capacity is defined as

$$\mathbf{C} = \max_{\mathbf{f(c)}} \mathbf{I(c;r)} \tag{2.4}$$

where $\mathbf{f(c)}$ is the probability distribution of the vector $\mathbf{c}$ and $\mathbf{I(c;r)}$ is the mutual information between the vectors $\mathbf{c}$ and $\mathbf{r}$.

The mutual information $\mathbf{I(c;r)}$ is given by

$$\mathbf{I(c;r)} = \log_2 \det(\mathbf{I_{n_R}} + \frac{E_s}{n_T N_0} \mathbf{HR_{cc}H}^H) \ \ bps/Hz \tag{2.5}$$

where $\mathbf{R_{cc}} = \varepsilon\{\mathbf{cc}^H\}$ is the covariance matrix of $\mathbf{c}$. E_s is the transmitter average power for one symbol period and $\varepsilon\{\mathbf{nn}^H\} = N_0 \mathbf{I}_{n_R}$.

Since the transmitters doe not know the channel $\mathbf{H}$, the transmit power is allocated such that all the n_T antennas transmit $\frac{N}{n_T}$ power where N is the total

transmit power. For unit transmit signal power, the covariance matrix is given by $\mathbf{R_{cc}} = \mathbf{I}_{n_T}$ and the capacity is

$$\mathbf{C_{EP}} = \log_2 \det(\mathbf{I_{n_R}} + \frac{E_s}{n_T N_0}\mathbf{HH}^H). \tag{2.6}$$

If r is the rank of the channel matrix $\mathbf{H}$ and $\lambda_i(i = 1, 2, \ldots, r)$ are the eigenvalues of $\mathbf{HH}^H$, the capacity for equal power allocation is given by

$$\mathbf{C_{EP}} = \sum_{i=1}^{r} \log_2(1 + \frac{E_s}{n_T N_0}\lambda_i). \tag{2.7}$$

The capacity of a MIMO system is equivalent to the sum of r SISO systems.

The figure below shows the capacity for different antenna configurations. For a 2×2 system the capacity, at 20 db SNR, is about 12 bps/Hz and the maximum data rate for a 20 MHz bandwidth is 240 Mbps. 1 Gbps could be reached for a 4×4 system with a bandwidth (BW) of 40 MHz.

2.4   Space Time Block Code

In [18], the authors presented a new transmit diversity technique which does not require any bandwidth expansion nor any feedback from the receiver to transmitter. The idea is to design an algorithm that can achieve maximum diversity gain with low decoding complexity.

The new scheme with 2×1 antennas has the same diversity order of a 1×2 maximum ratio combining (MRC) system.
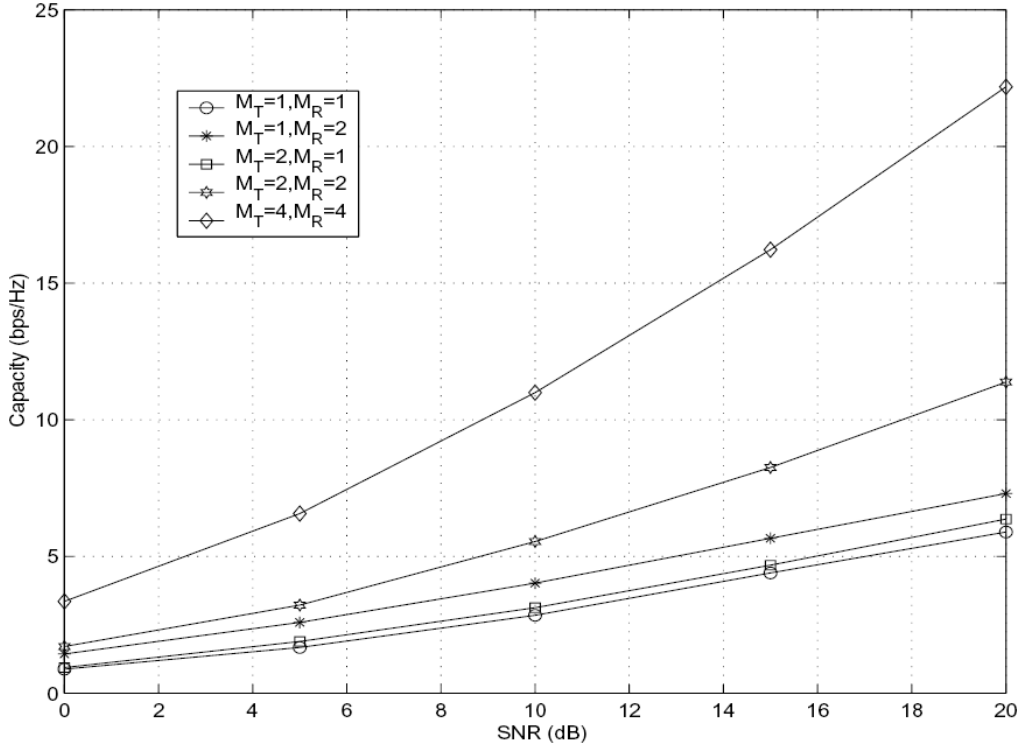
Figure 2.3: Capacity for different antenna configurations

The redundancy is obtained through space with the use of multiple antennas. The two-branch MRC is shown in the following figure 2.4.

The channel between the transmit antenna 1 and receive antenna 1 is $\mathbf{h_{11}}$ and 2 is $\mathbf{h_{12}}$. $\mathbf{c1}$ is sent from the transmit antenna 1. The receive signals are given by

$$\mathbf{r_1} = \mathbf{h_{11}c_1} + \mathbf{n_1} \tag{2.8}$$

$$\mathbf{r_2} = \mathbf{h_{12}c_1} + \mathbf{n_2} \tag{2.9}$$

where $\mathbf{n_1}$ and $\mathbf{n_2}$ are the complex Gaussian noises. The receiver two-branch MRC is given by

$$\tilde{\mathbf{c}}_1 = \mathbf{h_{11}^*r_1} + \mathbf{h_{12}^*r_2} \tag{2.10}$$
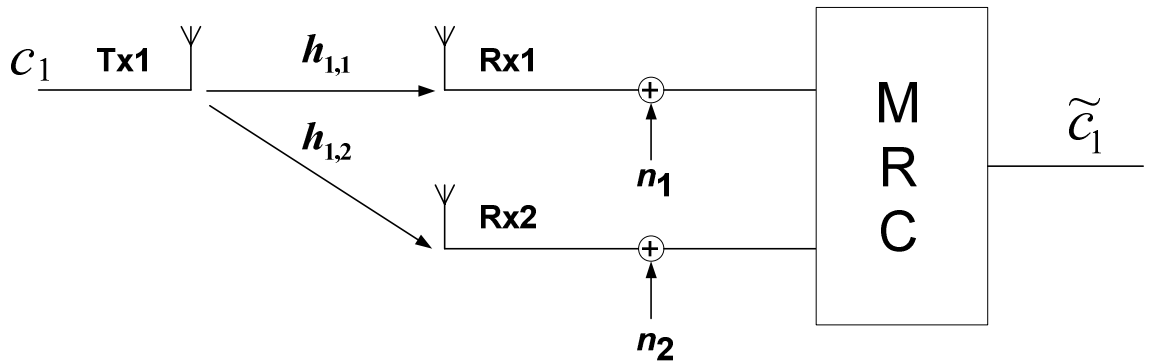
Figure 2.4: Two-branch MRC

For PSK signal constellation, the decision rule chooses $\mathbf{c_i}$ if and only if

$$d^2(\tilde{\mathbf{c}}_1, \mathbf{c_i}) = d^2(\tilde{\mathbf{c}}_1, \mathbf{c_k}) \quad \forall \, \mathbf{i} \neq \mathbf{k} \tag{2.11}$$

where

$$d^2(\mathbf{x}, \mathbf{y}) = (\mathbf{x} - \mathbf{y})(\mathbf{x}^* - \mathbf{y}^*). \tag{2.12}$$

The new transmit diversity scheme is described by the Fig. 2.5. During a symbol period, two signals are transmitted simultaneously from the Tx antenna 1 and 2. During the next symbol period, the signal $(-\mathbf{c_2^*})$ is transmitted from antenna 1 and $(\mathbf{c_1^*})$ from antenna 1 (see table 2.1).

With flat fading channel, the received signals are given by

$$\mathbf{r_1} = \mathbf{r}(t) = \mathbf{h_{11}c_1} + \mathbf{h_{21}c_2} + \mathbf{n_1} \tag{2.13}$$
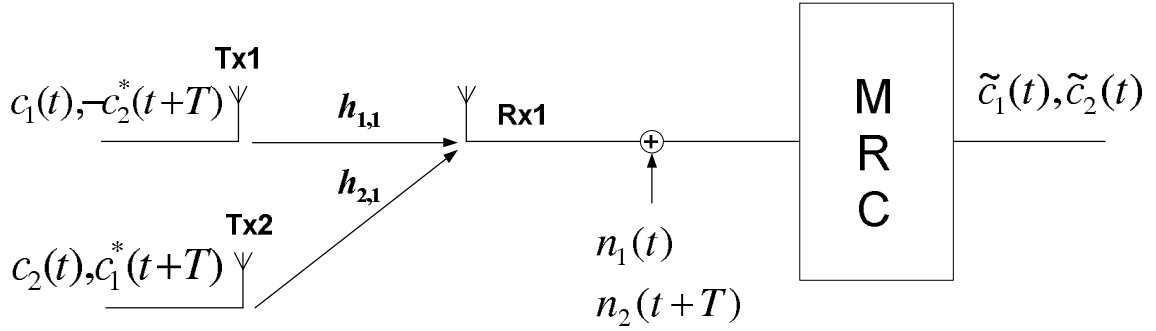
Figure 2.5: Two-branch transmit diversity scheme with one receiver

$$\mathbf{r_2} = \mathbf{r}(t+T) = -\mathbf{h_{11}c_2^*} + \mathbf{h_{21}c_1^*} + \mathbf{n_2} \qquad (2.14)$$

	$antenna0$	$antenna1$
$time\ \ t$	c_1	c_2
$time\ \ t+T$	$-c_2^*$	c_1^*

Table 2.1: Encoding and Transmission Sequence

Fig. 2.6 shows the BER performance of uncoded BPSK for MRC and the new Tx transmit diversity scheme. The total power for the new Tx scheme is the same as for the 1×2 MRC scheme. The diversity order for the 1×2 system is equal to the 2×1. The 3 dB loss is because the transmit power is only half the energy.

Tarokh et al., 1999 [19] extends STBC for more than two transmit antennas.

Figure 2.6: BER performance comparison of BPSK with MRC and two-branch transmit diversity in Rayleigh fading

2.5 Space-Time Convolutional Code

This section describes the basics of Space-Time Convolutional Code (STCC). We consider a wireless communication system utilizing n_T transmit and n_R receive antennas. A block error occurs when the decoded data sequence

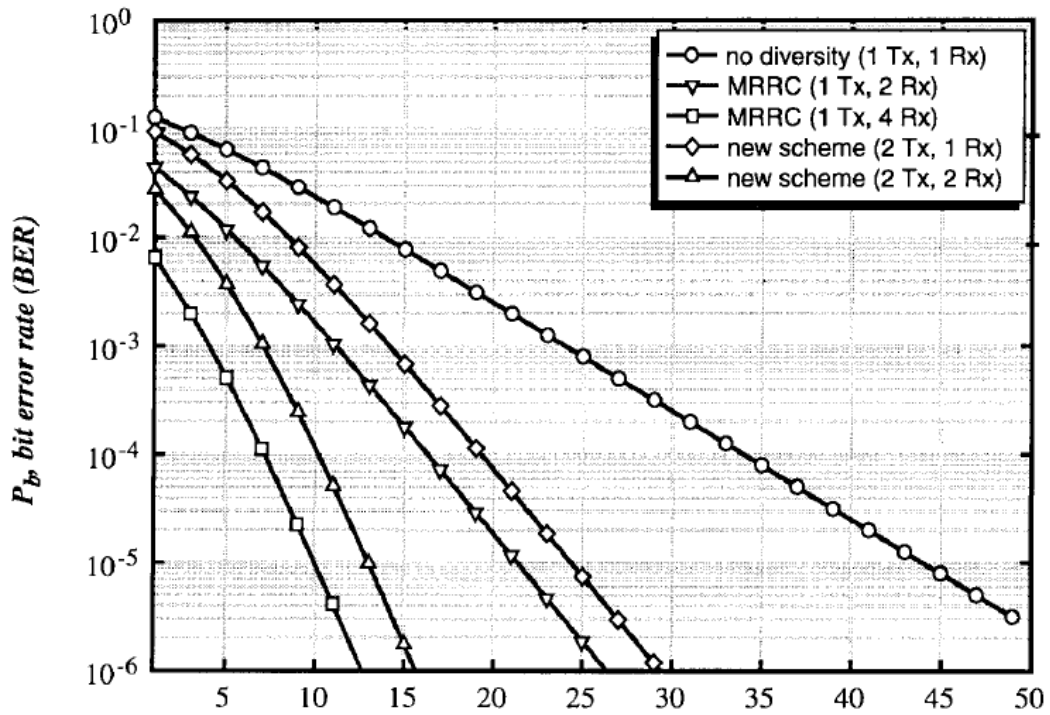$$\mathbf{e} = e_1^1 e_1^2 \ldots e_1^{n_T} e_2^1 e_2^2 \ldots e_2^{n_T} \ldots e_l^1 e_l^2 \ldots e_l^{n_T}$$

is different from the transmit data sequence

$$\mathbf{c} = c_1^1 c_1^2 \ldots c_1^{n_T} c_2^1 c_2^2 \ldots c_2^{n_T} \ldots c_l^1 c_l^2 \ldots c_l^{n_T}$$

where l is the number of symbols in one block. The channel path gain from antenna i to receive antenna j is denoted by $h_{i,j}$. These path gains are constant during a frame and change independently from one frame to another. The received data r_t^j at antenna j and time t, can be written as

$$r_t^j = \sum_{i=1}^{n_T} h_{i,j} c_t^i \sqrt{E_s} + n_t^j, \qquad 1 \leq j \leq n_R \tag{2.15}$$

where c_t^i is the complex transmit symbol with unit average power sent from antenna i at time t, n_t^j is the additive white Gaussian noise sample with zero mean and variance $\frac{N_0}{2}$ per dimension, and E_s is the signal energy.

The conditional pairwise block error probability has the upper bound [1]

$$P(\mathbf{c} \to \mathbf{e} \mid h_{i,j}, 1 \leq i \leq n_T, 1 \leq j \leq n_R) \leq$$
$$\exp\left(-d^2(\mathbf{c}, \mathbf{e}) \frac{Es}{4N_0}\right), \tag{2.16}$$

where $d^2(\mathbf{c}, \mathbf{e})$ is given by

$$d^2(\mathbf{c}, \mathbf{e}) = \sum_{j=1}^{n_R} \sum_{t=1}^{l} \left| \sum_{i=1}^{n_T} h_{i,j}(c_t^i - e_t^i) \right|^2 \qquad (2.17)$$

This upper bound on the pairwise block error probability can be written in matrix format as

$$P(\mathbf{c} \to \mathbf{e} \mid h_{i,j}, 1 \le i \le n_T, 1 \le j \le n_R) \le$$
$$\exp \left(\sum_{j=1}^{n_R} \Omega_j \mathbf{A} \Omega_j^* \frac{Es}{4N_0} \right), \qquad (2.18)$$

where $\Omega_j = [h_{1,j}, \ldots, h_{n_T,j}]$ and $\mathbf{A}(\mathbf{c}, \mathbf{e}) = \mathbf{B}(\mathbf{c}, \mathbf{e})\mathbf{B}^*(\mathbf{c}, \mathbf{e})$. The matrix $\mathbf{B}(\mathbf{c}, \mathbf{e})$ is defined as

$$\mathbf{B}(\mathbf{c}, \mathbf{e}) = \begin{pmatrix} e_1^1 - c_1^1 & \cdots & e_l^1 - c_l^1 \\ \vdots & \ddots & \vdots \\ e_1^{n_T} - c_1^{n_T} & \cdots & e_l^{n_T} - c_l^{n_T} \end{pmatrix}.$$

It is easy to show that the matrix $\mathbf{A}(\mathbf{c}, \mathbf{e})$ is a Hermitian matrix. Therefore, there is a unitary matrix V and a real diagonal matrix D such that $\mathbf{A}(\mathbf{c}, \mathbf{e}) = V^* D V$. The diagonal elements of D are the eigenvalues of $\mathbf{A}(\mathbf{c}, \mathbf{e})$ denoted as λ_i, $1 \le i \le n_T$.

Define a vector $\beta_{1,j}, \ldots, \beta_{n_T,j} = \Omega_j V^*$, then

$$\Omega_j \mathbf{A} \Omega_j^* = \sum_{i=1}^{n_T} \lambda_i |\beta_{i,j}|^2.$$

$|\beta_{i,j}|$ has a Rayleigh or Rican distribution depending on whether the channel paths have zero or non-zero mean distribution.

In the case of Rayleigh fading, the upper bound on the pairwise error proba-

bility of each block is further expressed as [1]

$$P(\mathbf{c} \to \mathbf{e}) \leq \left(\prod_{i=1}^{n_T} \frac{1}{1 + \frac{E_S}{4N_0}\lambda_i} \right)^{n_R} \tag{2.19}$$

In this paper, we assume that all the physical channel path gains are statistically independent with Rayleigh fading distribution. The extension of this work to Rician fading distribution is straightforward.

2.6 Construction of M-QAM Signal Constellation from QPSK Signals

The construction of M-QAM signal $(M = 2^{n_1})$ from multiple QPSK (x_i) signals can be obtained using the following equation [2, 3].

$$M - QAM = \sum_{i=1}^{\frac{n_1}{2}} 2^{i-1} \frac{\sqrt{2}}{2} x_i \exp\left(j\frac{\pi}{4}\right) \quad 1 \leq i \leq \frac{n_1}{2} \tag{2.20}$$

The QPSK modulation is realized by choosing x_i from the following set, $\{+1, +j, -1, -j\}$. In this equation, we use $\frac{n_1}{2}$ QPSK signals to construct an M-QAM symbol. Each M-QAM symbol that is constructed based on (2.20) uses the QPSK symbols obtained from the output of a QPSK STCC encoder. For example, to create a 16-QAM signal constellation from QPSK symbols, n_1 is equal to 4 in (2.20). In order to build a 16-QAM signal, we first apply rotation and scaling factors to the two QPSK signals x_0 and x_1 by multiplying them by $\exp(j\frac{\pi}{4})$ and $\frac{\sqrt{2}}{2}$. For the second operation, scaling factors of 2^0 and 2^1 are applied to x_0

and x_1 respectively. The third and final operation is a summation of the new scaled x_0 and x_1 constellations as shown in figure 2.7.

QPSK signal x0

Op 1

QPSK signal x1

Rotation
+ scale

Op 2

Scale

Op 3

Summation

16-QAM

x1, x0
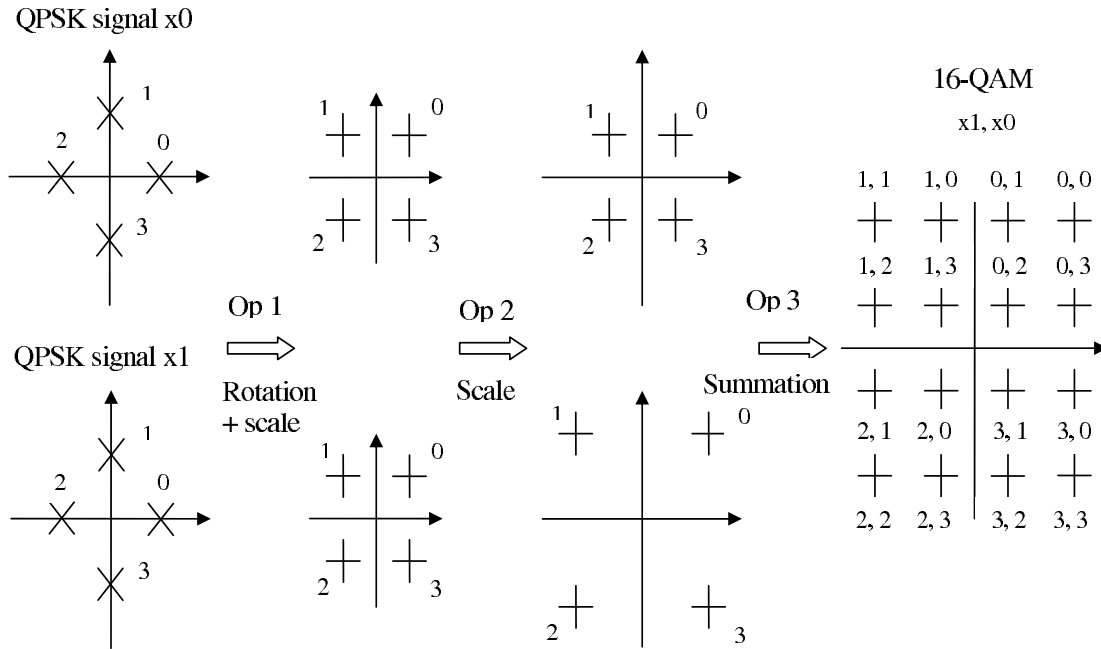
Figure 2.7: Construction of a 16-QAM signal constellation from two QPSK symbols

16

Chapter 3

Preliminary Works

3.1 Problem Formulation

The search space for STCCs increases exponentially with the increase in the con-
stellation size. However, utilizing QPSK STCC as component code, we can design
STCC with large constellation size without any need for such search. We will first
compute the diversity and coding gain with only a single transmit antenna by
creating virtual path gains as long as we have multiple receive antennas. The
construction of M-QAM STTCs with high spectral efficiencies will be done using
QPSK STCC based on (2.20).

$$r_t^j = \sum_{i=1}^{n_T} h_{i,j} C_t^i \sqrt{E_s} + n_t^j, \qquad 1 \le j \le n_R \qquad (3.1)$$

We propose to modify the transmit signal C_t^i using (2.20).

$$C_t^i = \sum_{v=1}^{n_V} 2^{v-1} \frac{\sqrt{2}}{2} c_t^v \exp\left(j\frac{\pi}{4}\right) \qquad (3.2)$$

n_V is the number of statistically dependent virtual path gains created between each transmit and receive antennas, and c_t^v are the symbols from the output of the STCC emcoder.

It is shown in [11] that an $n_T \times n_R$ MIMO system is equivalent of n_T distinct $1 \times n_R$ single-input multiple-output (SIMO) systems. Consequently, by sending C_t^i from each transmit antenna, we are creating an equivalent of parallel virtual MIMO systems.

Combining (3.1) and (3.2) leads to

$$r_t^j = \sum_{i=1}^{n_T} h'_{i,j} c_t^i \sqrt{E_s} + n_t^j, \qquad 1 \le j \le n_R \qquad (3.3)$$

with

$$h'_{i,j} = h_{i,j} \sum_{v=1}^{n_V} 2^{v-1} \frac{\sqrt{2}}{2} \exp\left(j\frac{\pi}{4}\right) \qquad (3.4)$$

Let's define $\Omega'_j = [h'_{1,j}, \ldots, h'_{n_T,j}]$ and

$$\beta'_{1,j}, \ldots, \beta'_{n_T,j} = \Omega'_j V^* \qquad (3.5)$$

then

$$\Omega'_j \mathbf{A} \Omega_j^{*\prime} = \sum_{i=1}^{n_T} \lambda'_i |\beta'_{i,j}|^2. \qquad (3.6)$$

The pairwise error probability, in case of Rayleigh fading, is expressed as

$$P(\mathbf{c} \to \mathbf{e}) \leq \left(\prod_{i=1}^{n_T} \frac{1}{1 + \frac{E_S}{4N_0}\lambda_i'} \right)^{n_R} \tag{3.7}$$

Assuming the number n_T of transmit antennas equals to 1, (2.15) becomes

$$r_t^j = h_{1,j} C_t \sqrt{E_s} + n_t^j. \qquad 1 \leq j \leq n_R \tag{3.8}$$

The coefficients $h_{1,j}$ are modeled as independent samples of complex Gaussian random variables with zero complex mean and variance 0.5 per dimension.

We have created a MIMO ($n_V \times n_R$) system from a SIMO ($1 \times n_R$) system. The actual number of physical channel path gains are n_R, therefore, the rank of the new channel matrix is unchanged. $d^2(\mathbf{c}, \mathbf{e})$ is now given by

$$d^2(\mathbf{c}, \mathbf{e}) = \sum_{j=1}^{n_R} \sum_{t=1}^{l} |h_{1,j}|^2 \left| \sum_{i=1}^{n_V} 2^{i-1} \frac{\sqrt{2}}{2} (c_t^i - e_t^i) \right|^2 \tag{3.9}$$

Equivalently, it can be written as

$$d^2(\mathbf{c}, \mathbf{e}) = \sum_{j=1}^{n_R} |h_{1,j}|^2 \, \mathbf{A}'(\mathbf{c}, \mathbf{e}), \tag{3.10}$$

where

$$\mathbf{A}'(\mathbf{c}, \mathbf{e}) = \sum_{t=1}^{l} \left| \sum_{i=1}^{n_V} 2^{i-1} \frac{\sqrt{2}}{2} (c_t^i - e_t^i) \right|^2. \tag{3.11}$$

The conditional pairwise block error probability can be upper bounded as

$$P(\mathbf{c} \rightarrow \mathbf{e} \mid h_{1,j}, 1 \leq j \leq n_R) \leq$$
$$\prod_{j=1}^{n_R} \exp\left(-|h_{1,j}|^2 \mathbf{A}'(\mathbf{c}, \mathbf{e}) \frac{Es}{4N_0}\right) \tag{3.12}$$

By averaging (3.12) with respect to independent Rayleigh distribution of $|h_{1,j}|^2$, we get

$$P(\mathbf{c} \rightarrow \mathbf{e}) \leq \left(1 + \mathbf{A}'(\mathbf{c}, \mathbf{e})\right)^{-n_R} \tag{3.13}$$

This result clearly demonstrates that in order to reduce the upper bound on the pairwise block error probability, we need to maximize the minimum Euclidean distance of the STCC. There are several techniques in literature to design STCC that maximizes the minimum Euclidean distance [5, 6, 7].

The QPSK STCC component code with 16 states, 2b/s/Hz will be taken from [7].

3.2   QPSK STCC Simulation Results

For this particular example, each STCC encoder contains 130 symbols which is equivalent of 520 bits per frame. The channel is Rayleigh fading channel and it is constant during each frame of 130 symbols and changes independently from one frame to another. A coherent detection is assumed at the receiver that requires perfect knowledge of the channel.

Figure 3.1 demonstrates the frame error rate performance of 2×3 and 2×5 MIMO systems utilizing 16-QAM STCC of [1] and the new scheme combining 2

QPSK STCCs of [7]. The simulation result demonstrates that the new scheme outperforms the existing 16-QAM STCC of [1] by as much as 2 dB.
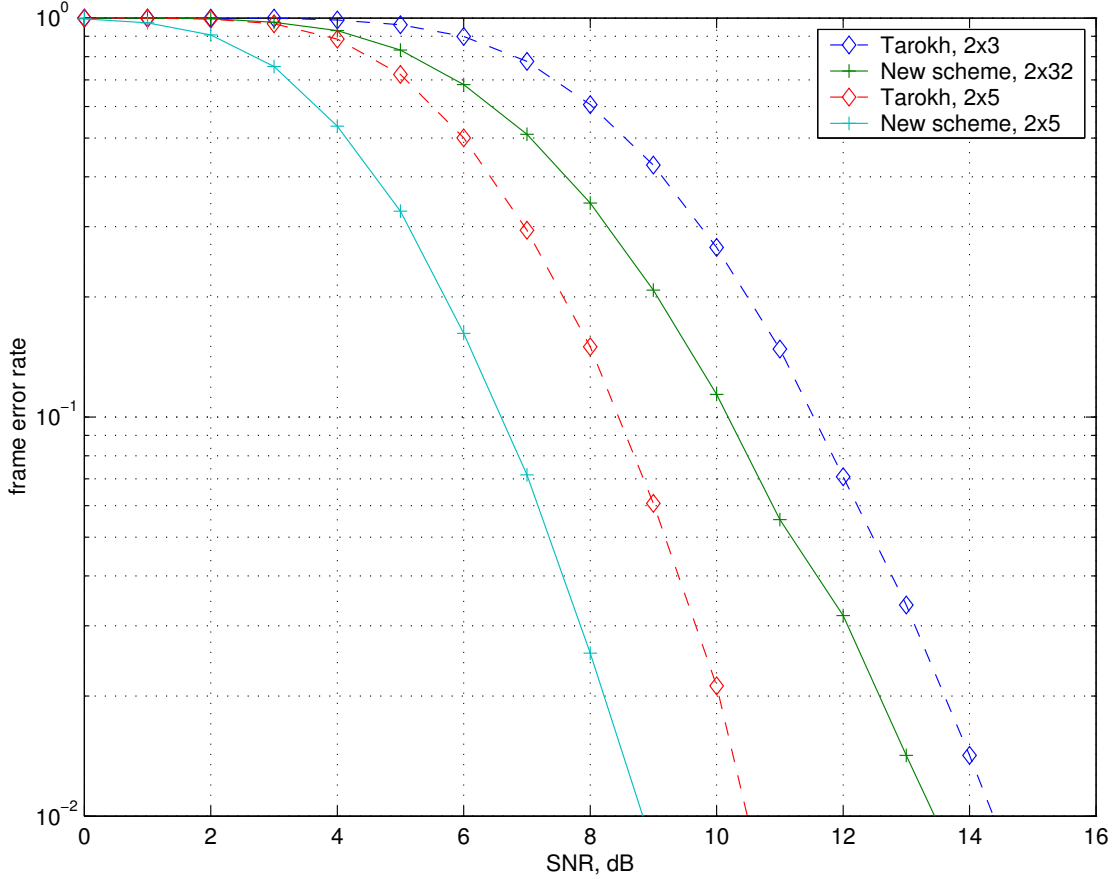
Figure 3.1: Frame error rate performance of a 16-QAM STCC 2×3 and 2×5 systems from [1] are compared with the new scheme using 16-QAM constellation constructed from two STCC QPSK of [7].

3.3 Combined Array Processing and STCC

In order to reduce the encoding and decoding complexity, [8] introduced a new combined array processing technique. Each output of the space-time encoder C_j is decoded separately while suppressing signals from other antennas.

Combining 3.1 and 3.2 leads to

$$r_t^j = \sum_{i=1}^{n_T} \sum_{v=1}^{n_V} h_{i,j}^v c_t^{v,i} \sqrt{E_s} + n_t^j, \qquad 1 \le j \le n_R \tag{3.14}$$

with

$$h_{i,j}^v = h_{i,j} 2^{v-1} \frac{\sqrt{2}}{2} \exp\left(j\frac{\pi}{4}\right). \tag{3.15}$$

Using vector notation, (3.14) is expressed as

$$\mathbf{r}_t = \Omega_v \mathbf{c}_t + \mathbf{n}_t, \tag{3.16}$$

where

$$\mathbf{c}_t = (c_t^1, c_t^2, \dots, c_t^{n_T})^T \tag{3.17}$$

$$\mathbf{r}_t = (r_t^1, r_t^2, \dots, r_t^{n_R})^T \tag{3.18}$$

$$\mathbf{n}_t = (n_t^1, n_t^2, \dots, n_t^{n_R})^T \tag{3.19}$$

and for the ith element of vector $\mathbf{c}_t$, we have

$$c_t^i = c_t^{1,i} c_t^{2,i} \dots c_t^{n_v,i}.$$

Ω_v is obtained by expanding the matrix elements $h_{i,j}$ of

$$\Omega = \begin{pmatrix} h_{1,1} & h_{2,1} & \dots & h_{n_T,1} \\ h_{1,2} & h_{2,2} & \dots & h_{n_T,2} \\ \vdots & \ddots & & \vdots \\ h_{1,n_R} & h_{2,n_R} & \dots & h_{n_T,n_R} \end{pmatrix} \tag{3.20}$$

using

$$h_{i,j} = (h_{i,j}^1, h_{i,j}^2, \ldots, h_{i,j}^{n_v}). \tag{3.21}$$

Ω_v has, therefore, n_R rows and $n_T \times n_v$ columns whereas (3.20) has n_T columns.

$$\Omega_v = \begin{pmatrix} h_{1,1}^1 \ldots h_{1,1}^{n_v} & \cdots & h_{n_T,1}^1 \ldots h_{n_T,1}^{n_v} \\ h_{1,2}^1 \ldots h_{1,2}^{n_v} & \cdots & h_{n_T,2}^1 \ldots h_{n_T,2}^{n_v} \\ \vdots & \ddots & \vdots \\ h_{1,n_R}^1 \ldots h_{1,n_R}^{n_v} & \cdots & h_{n_T,n_R}^1 \ldots h_{n_T,n_R}^{n_v} \end{pmatrix} \tag{3.22}$$

$\Theta_v(C_1)$ is formed by the set of orthonormal vectors in $\mathcal{N}$, where $\mathcal{N}$ is the *left null space* of the matrix $\Lambda_v(C_1)$. $\Lambda_v(C_1)$ is

$$\Lambda_v(C_1) = \begin{pmatrix} h_{n_1+1,1}^1 \ldots h_{n_1+1,1}^{n_v} & \cdots & h_{n_T,1}^1 \ldots h_{n_T,1}^{n_v} \\ h_{n_1+1,1}^2 \ldots h_{n_1+1,2}^{n_v} & \cdots & h_{n_T,2}^1 \ldots h_{n_T,2}^{n_v} \\ \vdots & \ddots & \vdots \\ h_{n_1+1,n_R}^1 \ldots h_{n_1+1,n_R}^{n_v} & \cdots & h_{n_T,n_R}^1 \ldots h_{n_T,n_R}^{n_v} \end{pmatrix} \tag{3.23}$$

The transmit antennas can be partitioned into q groups with $n_1+n_2+\ldots+n_q = n_T$.

By multiplying both side of the equation 3.16 by $\Theta_v(C_1)$,

$$\Theta_v(C_1)\mathbf{r}_t = \Theta_v(C_1)\Omega_v\mathbf{c}_t + \Theta_v(C_1)\mathbf{n}_t, \tag{3.24}$$

and since $\Theta_v(C_1)\Lambda_v(C_1) = 0$

$$\Theta_v(C_1)\mathbf{r}_t = \Theta_v(C_1)\Omega_v(C_1)\mathbf{c}_t^1 + \Theta_v(C_1)\mathbf{n}_t, \tag{3.25}$$

23

the received data can be expressed as

$$\tilde{\mathbf{r}}_\mathbf{t} = \tilde{\Omega}_v \mathbf{c}_t^1 + \tilde{\mathbf{n}}_\mathbf{t} \tag{3.26}$$

where

$$\tilde{\mathbf{r}}_\mathbf{t} = \Theta_v(C_1)\mathbf{r}_t \tag{3.27}$$

$$\tilde{\Omega}_v = \Theta_v(C_1)\Omega_v(C_1) \tag{3.28}$$

$$\tilde{\mathbf{n}}_\mathbf{t} = \Theta_v(C_1)\mathbf{n}_t \tag{3.29}$$

and

$$\Omega_v(C_1) = \begin{pmatrix} h_{1,1}^1 \dots h_{1,1}^{n_v} & \dots & h_{n_1,1}^1 \dots h_{n_1,1}^{n_v} \\ h_{1,2}^1 \dots h_{1,2}^{n_v} & \dots & h_{n_1,2}^1 \dots h_{n_1,2}^{n_v} \\ \vdots & \ddots & \vdots \\ h_{1,n_R}^1 \dots h_{1,n_R}^{n_v} & \dots & h_{n_1,n_R}^1 \dots h_{n_1,n_R}^{n_v} \end{pmatrix} \tag{3.30}$$

As an example, let's set $n_T = 2$, $n_R = 4$ and $n_V = 2$ corresponding to a 16-QAM constellation with spectral efficiency of 4 bits/s/Hz. Since we have only 2 transmit antennas, $n_1 = 1$. The first two bits of the input data are used by the encoder C_1 and the second two bits by the encoder C_2. The encoder $C_1 = C_2 = C$ is the 16-state 4-PSK STTC given in [1]. The output of encoder C_1 and C_2, which are 16-QAM symbols, will be transmitted by the antenna 1 and 2 respectively. The diversity order is equal to 8. The new diversity order for C_1, when applying the CAP technique has a diversity of 4.

Ω_v is given by

$$\Omega_v = \begin{pmatrix} h_{1,1}^1 & h_{1,1}^2 & h_{2,1}^1 & h_{2,1}^2 \\ h_{1,2}^1 & h_{1,2}^2 & h_{2,2}^1 & h_{2,2}^2 \\ h_{1,3}^1 & h_{1,3}^2 & h_{2,3}^1 & h_{2,3}^2 \\ h_{1,4}^1 & h_{1,4}^2 & h_{2,4}^1 & h_{2,4}^2 \end{pmatrix} \tag{3.31}$$

and $\Lambda_v(C_1)$ by

$$\Lambda_v(C_1) = \begin{pmatrix} h_{2,1}^1 & h_{2,1}^2 \\ h_{2,2}^1 & h_{2,2}^2 \\ h_{2,3}^1 & h_{2,3}^2 \\ h_{2,4}^1 & h_{2,4}^2 \end{pmatrix} \tag{3.32}$$

and $\Omega_v(C_1)$ by

$$\Omega_v(C_1) = \begin{pmatrix} h_{1,1}^1 & h_{1,1}^2 \\ h_{1,2}^1 & h_{1,2}^2 \\ h_{1,3}^1 & h_{1,3}^2 \\ h_{1,4}^1 & h_{1,4}^2 \end{pmatrix}. \tag{3.33}$$

The columns 2 and 4 of (3.31) will be a multiple of columns 1 and 3 respectively, and therefore the rank of Ω_v will be the same as Ω. Since $dim(\mathcal{N})+rank[\Lambda_v(C_1)] = n_R$, the rank of the *null space* will be 3 in this example. The receiver will first decode the symbols coming from the encoder $C1$ by nulling the output of the transmit antenna 2 and computing the decision metric [8]

$$\sum_{t=1}^{l} \left| (\tilde{\mathbf{r}}_\mathbf{t} - \tilde{\Omega}_v(C_1)\mathbf{c}_t^1) \right|^2 . \tag{3.34}$$

Once the receiver is done with the decoding of $C1$, the contributions of the codewords from the transmit antenna 1 are subtracted from the received signals and
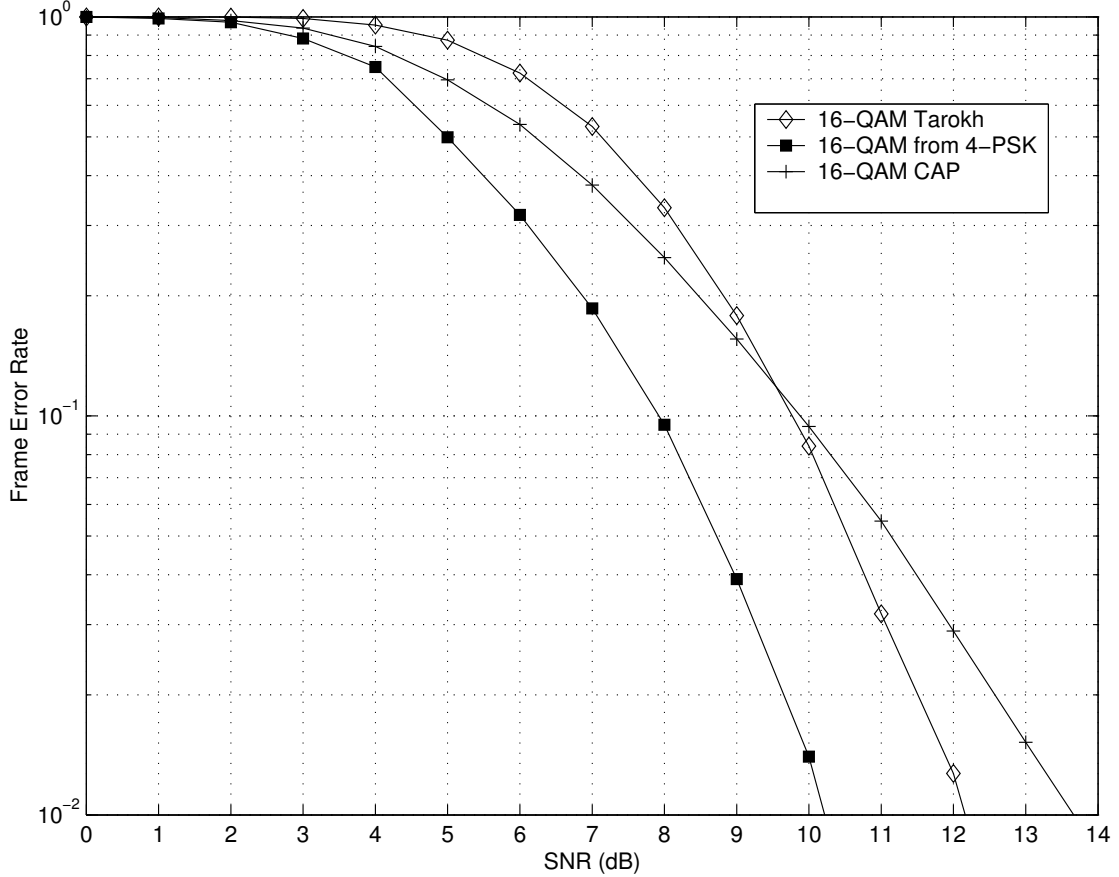
$C2$ decoded.

Figure 3.2: Frame error rate performance of a 16-QAM STCC 2×4 systems from Tarokh is compared with the CAP scheme using 16-QAM constellation constructed from two STCC QPSK

Figure 3.2 demonstrates the frame error rate performance of 16-QAM STCC 2×4 MIMO system with the CAP scheme utilizing 4-PSK component code from [1]. The complexity of product code is reduced for the CAP scheme from 256 to 32. The diversity order has been reduced as we can see from the slope of the curve. We are 2 dB away from the reference 16-QAM for a frame error rate of 10^{-1}.

3.4 Soft Decoding CAP for STCC

We proposed a new decoding scheme that can improve the previous results in figure 3.2 while maintaining the low complexity of the CAP algorithm. The new CAP technique uses a soft decoding method. The encoder for a M-QAM constellation is similar to that of [9].

Figure 3.4 shows the 4-PSK mapping from the input bits. The output of the encoder $C1$ is sent to the transmit antenna Tx1 and the output of the encoder $C2$ to Tx2 as shown by the figure 3.5. The encoding of the 4 bits/s/Hz takes place in 2 operations. The first operation generates the output of the encoder $C1$ (using the first symbol). The second operation generates the output of the encoder $C2$ (using the second symbol). Figure 3.7 shows the encoder trellis states and output symbols for the input stream from figure 3.4.

Figure 3.3: The 4-PSK constellation
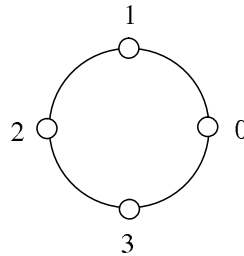
b0	b1	b2	b3	b4	b5	b6	b7
1	1	0	0	1	0	0	0
S0		S1		S2		S3	
3		0		1		0	

Figure 3.4: Example: input bits and corresponding 4-PSK symbols

Tx1   Tx2

C1		C2	
b0	b1	b2	b3
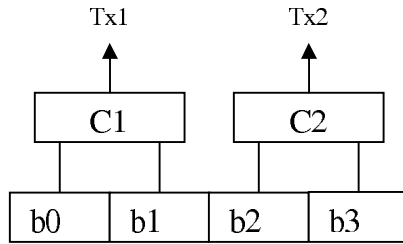
Figure 3.5: Encoder structure

```
 0     1     2     3
 +     +  |  +     +

 7     6  |  5     4
 +     +  |  +     +
_____|_____>

 +     +  |  +     +
 8     9  |  10    11

 +     +  |  +     +
15    14  |  13    12
```

Figure 3.6: 16-QAM constellation

4 b/s/Hz

S0 = 3	S1 = 0	S2 = 1	S3 = 0

(0) ——— (3) ——— (12) ——— (1) ——— (4)

| x0x1 = 03 | x0x1 = 32 | x0x1 = 23 | x0x1 = 12 |
| qam = 11 | qam = 14 | qam = 13 | qam = 8 |

Tx1   Tx2   Tx1   Tx2
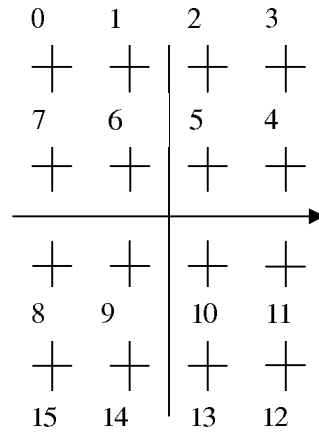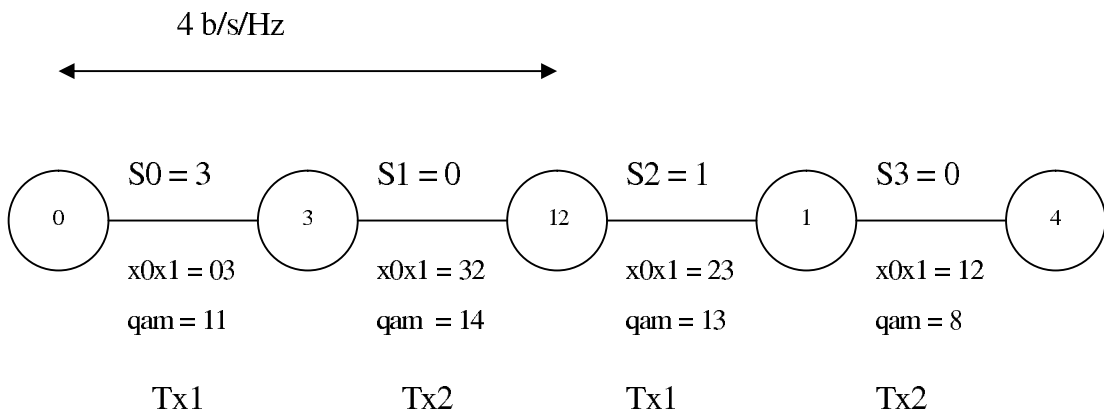
Figure 3.7: Trellis with input symbols and C_1 and C_2 encoder outputs

The decoding will start by the output of the encoder $C1$ as described in section 3.3. The $C1$ path metric is computed and the survivor path of each state is stored. Once all the $C1$ survivor paths are computed, the branch metrics for the output $C2$ is computed for each state by subtracting the codeword from the corresponding $C1$ survivor path. The best path from the encoder $C2$ is finally selected by computing the accumulated branch metrics using the soft decoding value from the encoder $C1$.
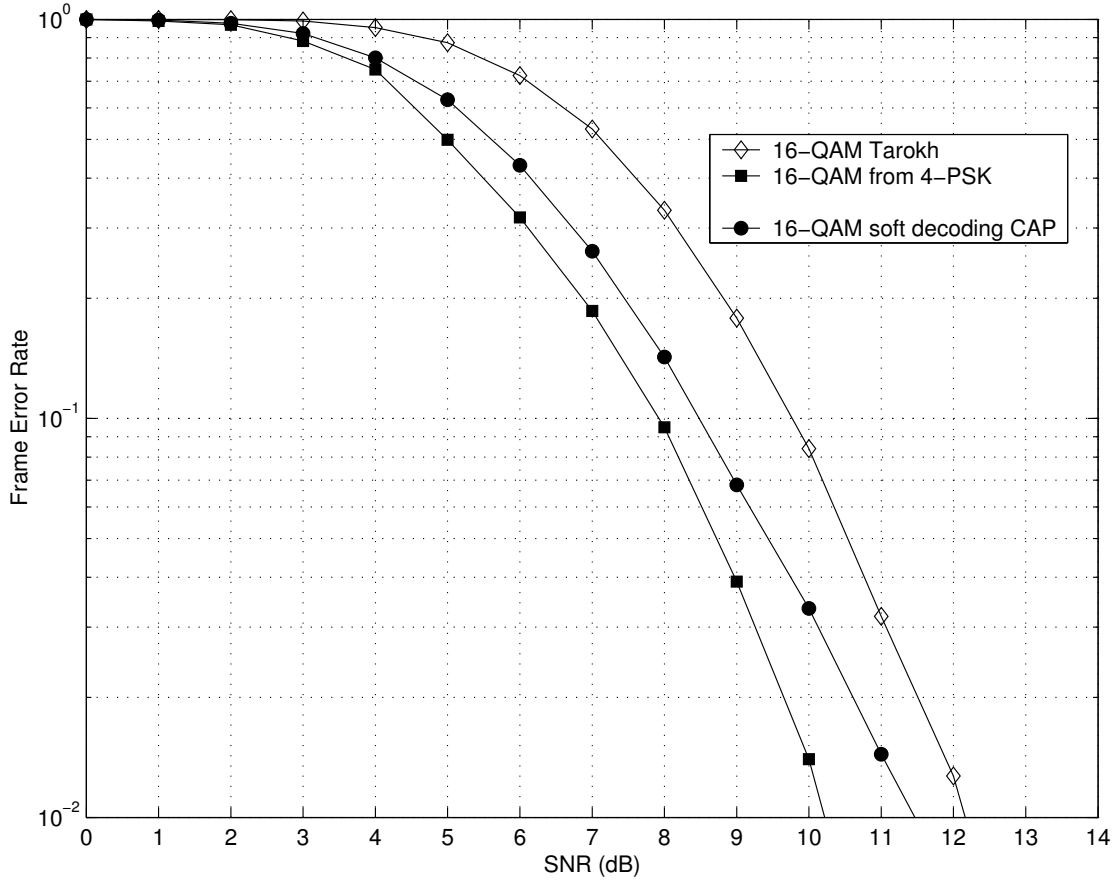

Figure 3.8: Frame error rate performance of a 16-QAM STCC 2×4 systems from Tarokh is compared with the new soft decoding CAP scheme using 16-QAM constellation constructed from two STCC QPSK

Figure 3.8 highlights the frame error rate performance of 16-QAM STCC 2×4

MIMO system with the new soft decoding CAP scheme utilizing 4-PSK component code from [1]. The decoding complexity of the soft decoding CAP is close to the original CAP scheme discribed in the section 3.3. For the frame error rate of 10^{-1}, we are only 0.5 dB away from the reference 16-QAM. It is obvious that the new CAP decoding algorithm has better diversity order.

Chapter 4

Future Research

This chapter presents the future research for a study on Space-Time Convolutional Code.

The construction of scalable M-QAM STCC could be improved to an optimum M-QAM if we choose optimized 4-PSK component codes, for example:

- for slow flat fading channels reported in [20];

- for fast flat fading channels in [21], [22] and [23];

- with trace design criteria derived in [24] or distance spectrum criteria in [25].

Moreover, the performance analysis of the new soft decoding CAP for STCC can be addressed as well, since the diversity order is, so far, only lower and upper bounded.

Our new technique could also address the MIMO-OFDM systems.

High throughput and reliable communication, for example high definition TV streaming, imposes the need for broadband channel up to 40 MHz compared to the narrow band channel that we have studied so far.

OFDM technique divides frequency selective channel (broadband) into sub-channels which become flat fading channels. The receiver complexity is greatly reduced by removing time domain equalizer.

Moreover, OFDM technique is well established for broadband applications like Wireless LAN as defined by the 802.11 a/g/n or by the 802.16e WiMax standard.

The creation of sub-channel is done by IFFT block. ISI is avoided by inserting a cyclic prefix (CP) at the transmitter with duration greater than the length of the channel response L. The receiver will remove the CP and recover the data by using a FTT block.

The diversity order for broadband channel is the product of the number of transmit antennas, the number of receive antennas and the frequency select order (L).

It has been shown in [28] that for example that Alamouti scheme [18] fails to achieve the full diversity and also, other ST codes [26] are only sub-optimal.

New criterion have been found in [27], [28], [29], [30]. Those new codes cannot ensure robust performance over different channel conditions (time delay of multi paths). This particular problem has been addressed by [31] and [32].

The application of our technique will allow us to extend the current 4-PSK codes to more complex constellations like 64-QAM, (already used in 802.11 and 802.16e standards).

Chapter 5

Conclusions

Since wireless channels have different paths between the transmitters and receivers, the receivers can be in deep fade. Transmit diversity can mitigate that problem along with other forms of diversity like time and frequency.

It has been shown that the capacity for MIMO channel increases with the number of antennas and is equivalent to the sum of r (r being the rank of the channel matrix) SISO channels.

STCC, which combines transmit diversity and coding, improves the reliability in wireless fading channel.

The first problem with STCC, we have addressed, is that the design of the transmit codewords is done by computer search (or by hand) and the complexity of the search grows exponentially with the number of transmit antennas as well with the constellation size. Only up to 16-QAM codewords have been published (as far as we know). We overcome that problem by using 4-PSK component codes

to construct M-QAM square constellation by using the following equation [2, 3].

$$M - QAM = \sum_{i=1}^{\frac{n_1}{2}} 2^{i-1} \frac{\sqrt{2}}{2} x_i \exp\left(j\frac{\pi}{4}\right) \quad 1 \leq i \leq \frac{n_1}{2} \tag{5.1}$$

The new 16-QAM scheme outperforms the existing 16-QAM STCC of [1] by as much as 2 dB (see figure 3.1).

The second problem with STCC, we have addressed, is that the complexity of the receiver grows exponentially with the number of antennas (diversity order) and the constellation size (or the number of bits/Hz of the coded symbol).

We reduced the complexity of the encoder and decoder by using a new group of interference cancellation technique also known as combined array processing (CAP). The complexity of our low decoding algorithm allows the decoding complexity to increase linearly by the number of transmit antennas. Moreover, the new method of soft decoding CAP keeps the performances (coding and diversity order) of the system (see figure 3.8) close to the more complex decoder. Indeed, for the frame error rate of 10^{-1}, we are only 0.5 dB away from the reference 16-QAM.

Bibliography

[1] V. Tarokh, N. Seshadri, and R. Calderbank, "Space-Time Codes for High Data Rate Wireless Communications: Performance Criterion and Code Construction," *IEEE Transaction on Information Theory*, vol. 44, pp. 744-765, March 1998.

[2] C. Röβing and V. Tarokh, "A Construction of OFDM 16-QAM Sequences having Low Peak Powers," *IEEE Transaction on Information Theory*, vol. 47, no. 5, pp. 2091-2094, July 2001.

[3] B. Tarokh, H.R. Sadjadpour, "Construction of OFDM M-QAM sequences with low peak-to-average power ratio," *IEEE Transaction on Communications,* vol. 51, pp. 25-28, January 2003.

[4] B. Tarokh, H.R. Sadjadpour, "Construction of OFDM M-QAM sequences with Low Peak to Average Power ratio," *IEEE CISS2001*, John Hopkins University, March 21-23, 2001.

[5] Z. Chen, J. Yuan, and B. Vucetic, *"An Improved Space-time Trellis Coded Modulation Scheme on Slow Rayleigh Fading Channels,"* IEEE International Conference on Communications, pp. 1110 - 1116, June 2001.

[6] J. Yuan, Z. Chen, B. Vucetic, and W. Firmanto, *"Performance and Design of Space-time Coding in Fading Channels,"* IEEE Transaction on Communications, vol. 51, pp. 1991-1996, December 2003.

[7] Q. Yan and R. S. Blum, *Improved space-time convolutional codes for quasi static slow fading channels,"* IEEE Transactions on Wireless Communications, pp. 563-571, Oct. 2002.

[8] V. Tarokh, A. Naguib, N. Seshadri, and R. Calderbank, "Combined Array Processing and Space-Time Coding," *IEEE Transaction on Information Theory*, vol. 45, NO. 4, May 1999.

[9] C. Rouchy and H.R. Sadjapour, "Construction of M-QAM STCC Based on QPSK STCC," *ICASSP 2006 Conference.*

[10] P.W. Wolniansky, G.J. Foschini, G.D. Golden, and R.A. Valenzuela, "V-BLAST: An architecture for realizing very high date rates over the rich-scattering wireless channels," *Proceedings of ISSSE,* Pisa, Italy, pp. 295-300, September 1998.

[11] H. R. Sadjadpour, K. Kim, H. Wang, R. Blum, and Y. Lee, "Application of randomization techniques to space-time convolutional Codes," IEEE WirelessCom 2005 and also accepted to IEEE Transactions on Signal Processing.

[12] Christophe Rouchy and Hamid Sadjadpour, "Construction of Space-time Convolutional Codes with High Spectral Efficiency," *39th Asilomar Conference on Signals, Systems and Computers*, Monterey, CA November 2005.

[13] Hamid Jafarkhani, "Space-Time Coding, Theory and Practice," *Cambridge University Press*, 2005.

[14] Christophe Rouchy and Hamid Sadjadpour, "Systematic Design of Space-Time Convolutional Codes," *42th Asilomar Conference on Signals, Systems and Computers*, Monterey, CA October 2008.

[15] Arogyaswami Paulraj, Rohit Nabar and Dhananjay Gore, "Introduction to Space-Time Wireless Communications," *Cambridge University Press*, 2003.

[16] E. Telatar, "Capacity of Multi-antenna Gaussian channels," *European Transactions on Telecommunications*, Nov./Dec. 1999.

[17] G.J. Foschini and M.J. Gans, "On Limits of Wireless Communications in a Fading Environment when Using Multiple Antennas," *Wireless Pers. Commun*, pp. 311-35, Mar. 1998.

[18] S. Alamouti, "A simple transmitter diversity scheme for wireless," *IEEE Journal on Selected Areas in Communications*, pp. 1451-8, Oct. 1998.

[19] V. Tarokh, H. Jafarkhani and A. R. Calderbank, "Space-time block codes from orthogonal designs," *IEEE Trans. on Information Theory*, pp. 1456-67, July 1999.

[20] S. Baro, G. Bauch, and Hansmanna, "Improved codes for space-time trellis-coded modulation," *IEEE Commun, Letters*, pp. 20-22, January 2000.

[21] J. Zhang, Y. Qiang, J. Wang, and D. Li, "On the design of space-time codes for fast fading channels," *Proc. IEEE PIMRC'03*, pp. 1045-1048, Sept. 2003.

[22] W. Firmanto, B.S. Vucetic, and J. Yuan, "Space-time TCM with improved performance on fast fading channels," *IEEE Commun. Letters*, pp. 154-156, April 2001.

[23] Y. Sasazaki and T. Ohtsuki, "Improved Design criteria and new trellis codes for space-time trellis coded modulation in fast fading channels," *IEICE Trans. on Commun.*, pp. 1057-1062, March 2003.

[24] M. Tao and R.S. Cheng, "Improved Design criteria and new trellis codes for space-time coded modulation in slow flat fading channels," *IEEE Commun. Letters*, pp. 313-315, July 2001.

[25] Y. Sasazaki and T. Ohtsuki, "Improved Design criteria and new codes on space-frequency trellis coding over frequency selective fading channel," *Proc. IEEE VTC'02-Fall*, pp. 2187-2191, Oct. 2002.

[26] Daskshi Agrawal, Vahid Tarokh, Ayman Naguib and Nambi Seshadri, "Space-Time Coded OFDM for High Data-Rate Wireless Communication Over Wideband Channels," *IEEE VTC'98*, pp. 2232-2236, 1998.

[27] Ben Lu and Xiaodong Wang, "Space-Time Code Design in OFDM Systems," *IEEE GLOBECOM*, pp. 1000-1004, November 2000.

[28] Helmut Bolcskei and Arogyaswami J. Paulraj, "Space-Frequency Coded Broadband OFDM Systems," *IEEE Wireless Communications and Networking Conference (WCNC)*, pp. 1-6, September 2000.

[29] Zhiqiang Liu, Yan Xin and Georgios B. Giannakis, "Space-Time-Frequency Coded OFDM Over Frequency-Selective Fading Channels," *IEEE Trans. on Signal Processing*, pp. 2465-2476, October 2002.

[30] Zihua Guo, Wenwu Zhu, and Khaled Ben Letaief, "Space-Frequency Trellis Coding for MIMO OFDM Systems," *IEEE Vehicular Technology Conference*, pp. 557-561, April 2003.

[31] Yi Hong, Jinhong Yuan, and Xun Shao, "Robust Space-Time Trellis Codes for OFDM Systems over Quasi-static Frequency Selective Fading Channels," *Proc. IEEE Personal, Indoor and Mobile Radio Communication (PIMRC)*, pp. 434-438, September 2003.

[32] Shouyin Liu and Jong-Wha Chong, "Improved Design Criterion for Space-Frequency Trellis Codes in MIMO-OFDM Systems," *IEEE Vehicular Technology Conference (VTC)*, pp. 1391-1395, September 2004.

[33] Rick S. Blum, Ye (Geoffrey) Li, Jack H. Winters, and Qing Yan, "Improved Space-Time Coding for MIMO-OFDM Wireless Communications," *IEEE Trans. on Communications*, Vol 49, pp. 1873-1878, November 2001.